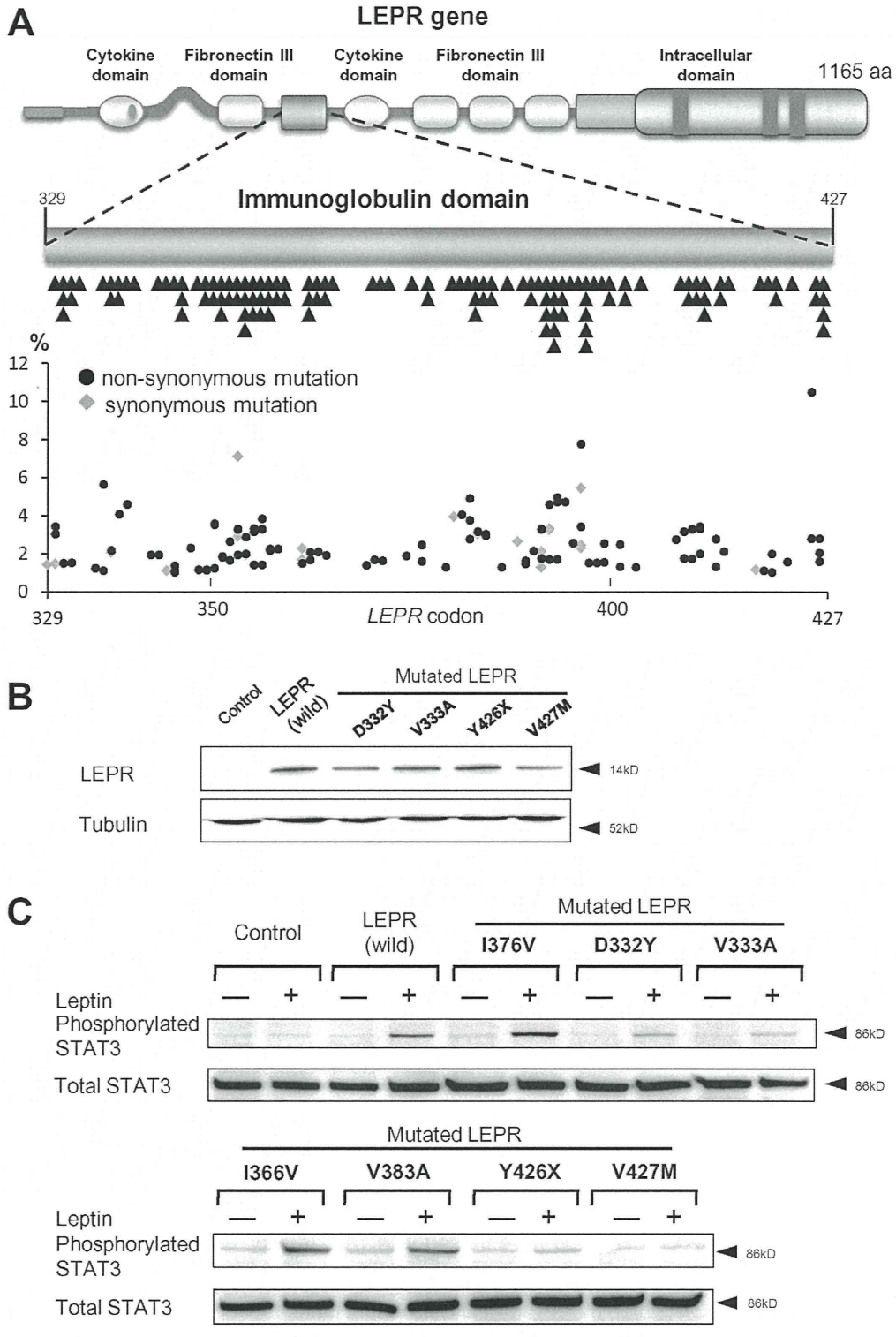

Figure 3. Distribution of mutations in the *LEPR* sequence in HCV-positive cirrhotic liver tissues. (*A*) Schematic diagram of the LEPR gene (*top panel*) and the Ig domain (*middle panel*). Mutated positions in the Ig domain are indicated by *black triangles*. A total of 38 of 67 (56.7%) mutated nucleotide positions of the Ig domain were recurrently mutated in 2 or more HCV-positive cirrhotic liver tissues. Frequencies of nonsynonymous (*black circles*) and synonymous (*gray diamonds*) mutations at each nucleotide position of the Ig domain of each sample are shown (*lower panel*). Nonsynonymous mutations were detected at 62 of the 67 nucleotide positions. (*B* and *C*) HEK293 cells were transfected with constructs encoding wild-type or representative various mutated *LEPR*s that were identified in HCV-positive cirrhotic liver tissues. Control: empty vector. (*B*) Immunoblotting was performed on the lysate of the cells expressing either wild-type or a mutated Ig domain (D332Y, V333A, Y426X, and V427M) of the *LEPR* gene using anti-Myc antibodies. (*C*) After transfection, the cells were treated with or without recombinant leptin protein. Total protein was isolated and immunoblot analysis was performed using anti–phospho-STAT3 (*upper panel*) and anti–total STAT3 (*lower panel*).

examination revealed the accumulation of lipids within individual hepatocytes in the *db/db* mouse liver, a typical feature of steatosis (Figure 4*A*).

After administering TAA, blood levels of alanine aminotransferase were substantially elevated in *db/db* mice compared with control mice (Supplementary Table 10). Consistently, histological examination revealed that inflammatory activity was more severe in the liver of *db/db* mice than in the liver of control mice (Figure 4*B*). None of the control mice treated with TAA showed tumorigenesis 24 weeks after administration of TAA. In contrast, macroscopic liver nodules developed in 4 of 10 (40%) *db/db* mice

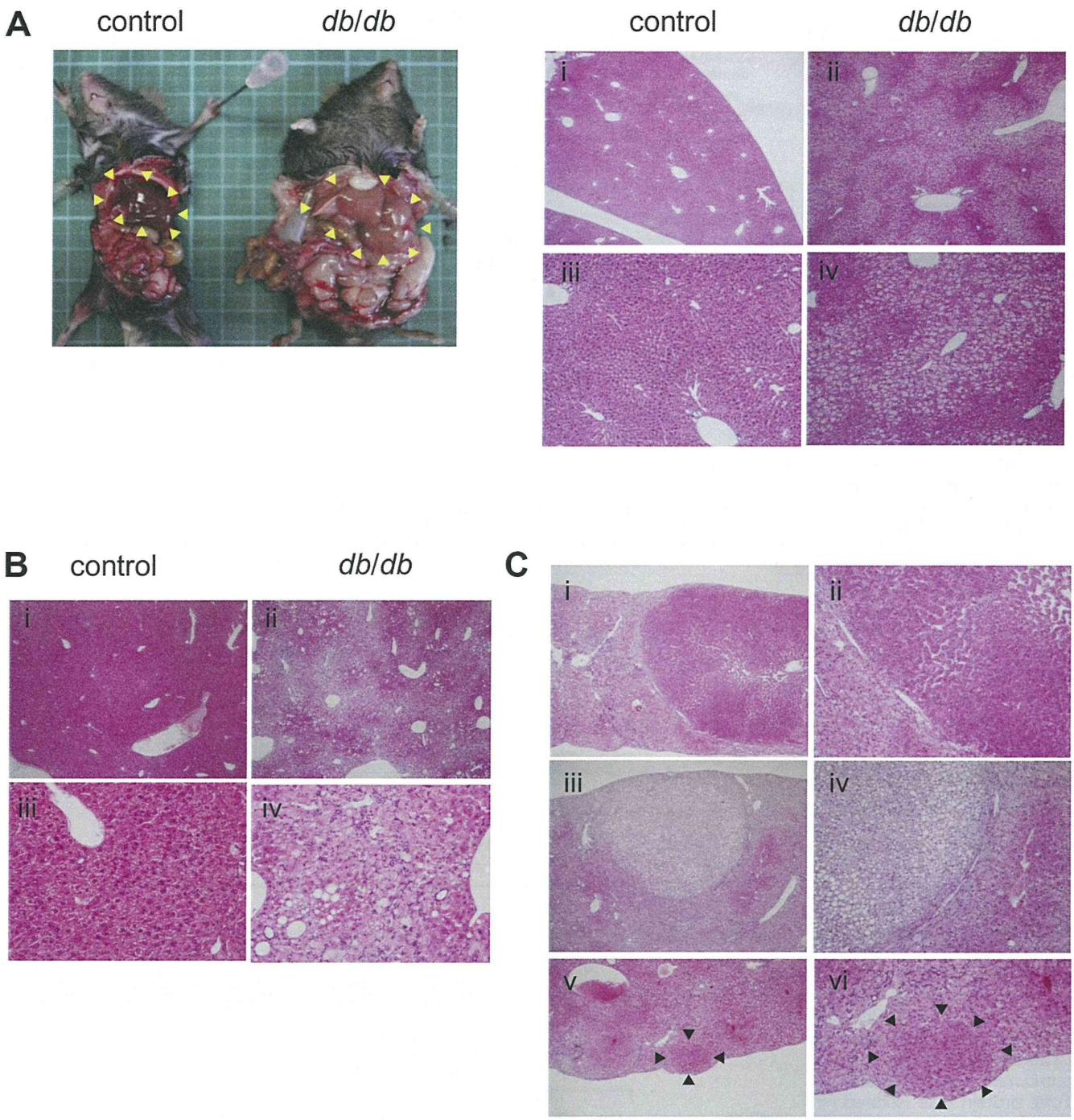

Figure 4. Tumors developed in *db/db* mice treated with TAA. (*A*) Representative macroscopic (*left panel*) and microscopic (*right panel*) images (H&E stain) of the liver from a *db/db* mouse and a littermate control mouse without administration of TAA. The liver of the *db/db* mouse is enlarged and yellowish compared with the control (*yellow arrowheads*). Histological analysis of the liver tissue of (*ii* and *iv*) *db/db* mouse and (*i* and *iii*) control mouse. Original magnification: 4× (*upper panels*) and 10× (*lower panels*). (*B*) Microscopic images (H&E stain) of (*i* and *iii*) control mice and (*ii* and *iv*) *db/db* mice treated with TAA for 24 weeks. In the *db/db* mice, inflammatory cell infiltration was extensively observed in the liver tissues underlying prominent steatosis (*ii* and *iv*). Original magnification: 4× (*upper panels*) and 20× (*lower panels*). (*C*) Microscopic images (H&E stain) of nodules that developed in *db/db* mice treated with TAA for 24 weeks (*i–vi*). Liver cancers developed in 2 *db/db* mice (*i–iv*). *Arrowheads* indicate hepatocyte hyperplasia (*v* and *vi*). Original magnification: 4× (*left panels*) and 10× (*right panels*).

that received the same dose of TAA during the same observation period (Table 2). Histological examination revealed that 2 *db/db* mice with liver nodules developed well-differentiated HCC (Figure 4*C*). In addition, the remaining nodules that developed in *db/db* mouse liver showed features of hepatocyte hyperplasia. These findings

Table 2. Incidence of Hepatic Nodules in C57BL/KsJ-*db/db* (*db/db*) and Misty (Control) Mice After 24 or 30 Weeks of Treatment With TAA

	db/db	Control
24 wk	n = 10	n = 10
Male/female	8/2	8/2
Tumor formation		
Total (%)	4[a] (40)	0 (0)
HCC	2	0
Hepatocyte hyperplasia	3	0
30 wk	n = 7	n = 10
Male/female	3/4	7/3
Tumor formation		
Total (%)	6[a] (86)	4 (40)
HCC	1	0
Hepatocyte hyperplasia	6	4

NOTE. The numbers of animals that developed hepatocyte hyperplasia and/or HCC are shown.
[a]One *db/db* mouse developed both HCC and hepatocyte hyperplasia.

suggest that Lepr-deficient *db/db* mice had high susceptibility to TAA-induced liver tumorigenesis.

Discussion

Tumor cells are considered to be generated by a stepwise accumulation of genetic alterations in tumor-related genes during the process of inflammation-associated carcinogenesis. Several studies have reported that epithelial tissues exposed to chronic inflammation accumulate genetic alterations in tumor-related genes before the onset of tumorigenesis.[7,8] Given that chronic inflammation induces somatic mutations, it is reasonable to assume that critical genetic alterations that contribute to tumorigenesis might emerge in chronically inflamed epithelial cells. Using whole exome sequencing, we showed here that considerable levels of somatic mutations accumulate not only in tumors but also in the nontumorous liver of patients with HCV-related cirrhosis.

Whole exome sequencing on synchronously developed HCCs showed a remarkable difference in the mutation signature in each case. In 2 cases, more than 20% of the mutated genes were commonly present in 2 tumors that developed in the same background liver, suggesting that these tumors were derived from a common origin or developed through intrahepatic metastasis. In contrast, the tumors that developed in the remaining case shared no common mutations, suggesting independent development in a multicentric manner. The data obtained from the latter case are consistent with those of a recent study in which no common somatic mutations were identified in the 2 pairs of multicentric HCCs that developed in the same background livers.[19] Taken together, these findings suggest that comprehensive whole exome sequencing on synchronously developed HCCs would permit distinction of the carcinogenic process between tumors that develop in a multicentric manner and that develop through intrahepatic metastasis.

Interestingly, we found that in some cases the total number of mutated genes of nontumorous liver tissues was larger than that of the matched tumor tissues, possibly due to the abundance of heterogeneous accumulation of passenger mutations in the nontumorous liver tissues.[30] The observation that the frequency of mutations at each nucleotide position in the nontumorous tissues tended to be lower than that in the matched tumor tissues may lend support to such a possibility. Notably, somatic mutations in the representative tumor-related genes, *TP53* and *CTNNB1*, were also latently accumulated in the cirrhotic liver tissues. It is unknown whether the *TP53* and/or *CTNNB1* mutations detected in nontumorous tissues were derived from the clinically undetectable small nest of cancer cells or premalignant hepatocytes; however, it is possible that these latent genetic alterations in tumor driver genes contribute to the development of HCC in the background of chronic liver disease.

Among the various mutated genes in the cirrhotic liver tissue, we identified *LEPR* as one of the most recurrently mutated genes. Indeed, we confirmed a total of 650 low-frequency mutations of the *LEPR* gene in 12 of 22 patients (54.5%) with HCV infection using selected exome sequencing. At present, it is not clear why a large number of mutations accumulate in the *LEPR* gene of nontumorous cirrhotic liver in patients with chronic HCV infection. One possibility may be that the *LEPR* gene is highly sensitive to AID-mediated mutagenesis in hepatocytes, because we recently observed that AID activation in cultured hepatoma-derived cells preferentially caused somatic mutations in the *LEPR* gene (Supplementary Table 11). On the other hand, close attention must be paid to the fact that only low-frequency mutations were detected in the *LEPR* gene in tumor tissues, consistent with the reported cancer genome database (International Cancer Genome Consortium data set version 12; http://dcc.icgc.org/web/). In general, tumor-specific driver mutations in tumor tissues are characterized by high-frequency mutations (eg, more than 20% nucleotide changes of total reads[18,23,31]). In this regard, the frequency of any mutation in the *LEPR* gene observed in the tumor tissues was more than 20% in our cases. Thus, the genetic changes in LEPR are unlikely to be direct driver mutations for HCC, but rather might play some role in the development of HCC in HCV-infected inflamed liver by providing a pathophysiological background for hepatocarcinogenesis by modifying the cell proliferation activity.

Leptin is a circulating hormone that is secreted by adipocytes and regulates energy homeostasis.[32] Leptin acts through binding to the extracellular domain of specific membrane receptor LEPR, which belongs to a family of class I cytokine receptors.[33] The extracellular domain of LEPR comprises 2 canonical cytokine receptor homology domains, Ig and fibronectin III domains, and the Ig domain is essential for the formation of the hexameric complex and for receptor activation.[34] In the present study, we confirmed that 67 mutations were present in the Ig domain

of *LEPR* in cirrhotic liver, and more than half of the mutations were recurrently mutated in 2 or more patients. Notably, more than 90% of those nucleotide alterations that accumulated in the Ig domain of *LEPR* were nonsynonymous mutations. Furthermore, we revealed that several nonsynonymous mutations that appeared in the Ig domain of *LEPR* impaired signaling to STAT3 in response to leptin, causing dysregulation of leptin signaling in the cells with those mutations. Sequencing the *LEPR* gene in patients with severe early-onset obesity revealed that the extracellular region of the LEPR has a variety of mutations in those patients.[35] A functional study of missense mutations in the *LEPR* found in severely obese patients also revealed that mutated LEPR has impaired signaling to STAT3, which is consistent with their inability to activate pathways involved in the reduction of food intake.[36] Together, these findings suggested that somatic mutations in the *LEPR* gene might provide the genetic basis for developing metabolic dysregulation in hepatocytes during hepatocarcinogenesis.

In the present study, we showed for the first time that *db/db* mice with disruption of the Lepr gene were more susceptible to developing hepatic inflammation as well as TAA-mediated tumorigenesis than wild-type mice. Consistent with our findings, a previous study reported an increased incidence of hepatocyte hyperplasia in leptin-deficient *ob/ob* mice, a model for nonalcoholic fatty liver disease.[37] Taken together, it is strongly suggested that dysregulation of LEPR signaling has a role in hepatic tumor development, but the mechanism of how the leptin signaling deficiency contributes to an enhanced inflammatory response and tumorigenesis is currently unknown. It should be noted that both *ob/ob* mice and *db/db* mice are characterized by hepatic steatosis, and steatosis is well recognized as a common histopathologic feature of the chronic HCV-infected liver. Epidemiological studies have revealed that fatty liver disease may be a common underlying pathology in patients with HCC,[38,39] and steatosis is an important cofactor in accelerating the development of hepatic fibrosis and inflammatory activity,[40,41] contributing to the progression of HCC in HCV-related chronic liver disease.[42] We found no correlation between the prevalence of *LEPR* mutations and the histological feature of fatty changes in HCV-positive cirrhotic liver tissues. On the other hand, previous studies have shown that leptin can oppose the action of insulin-induced signaling by reducing the phosphorylation of insulin receptor substrate 1 in human hepatic cells.[43,44] In addition, it was shown that leptin suppresses HCC via activation of the immune response, suggesting the tumor-suppressing function of leptin-mediated signaling.[45] Thus, we speculate that dysregulation of leptin signaling in the liver might be involved in the neoplastic process of patients with HCV-related chronic liver damage. Because somatic mutations in *LEPR* are limited to a small proportion of cells in cirrhotic liver tissue and the TAA-mediated liver inflammation model does not fully recapitulate HCV-associated chronic liver disease, further analysis is required to determine whether dysregulation of LEPR-mediated signaling caused by *LEPR* mutations contributes to the enhanced inflammatory response or tumorigenesis in patients with HCV-related chronic liver damage.

In conclusion, we showed that various somatic mutations latently accumulate in the nontumorous cirrhotic liver of patients with HCV infection. The findings that the *LEPR* gene was recurrently mutated in cirrhotic liver provide a novel putative link between the inflammation-mediated genetic aberrations, the dysregulation of leptin signaling, and the development of HCC in patients with HCV-related chronic liver disease. The gene catalogue identified in the HCV-infected chronically damaged liver might contain the putative driver gene associated with tumor initiation as well as the gene that provides the genetic basis for the development of HCC. Thus, further studies are required to identify the genetic alterations that contribute to tumor development in chronically inflamed liver underlying chronic HCV infection.

Supplementary Material

Note: To access the supplementary material accompanying this article, visit the online version of *Gastroenterology* at www.gastrojournal.org, and at http://dx.doi.org/10.1053/j.gastro.2013.09.025.

References

1. Coussens LM, Werb Z. Inflammation and cancer. Nature 2002;420:860–867.
2. Chiba T, Marusawa H, Ushijima T. Inflammation-associated cancer development in digestive organs: mechanisms and roles for genetic and epigenetic modulation. Gastroenterology 2012;143:550–563.
3. Lengauer C, Kinzler KW, Vogelstein B. Genetic instabilities in human cancers. Nature 1998;396:643–649.
4. Hanahan D, Weinberg RA. The hallmarks of cancer. Cell 2000;100:57–70.
5. Hussain SP, Schwank J, Staib F, et al. TP53 mutations and hepatocellular carcinoma: insights into the etiology and pathogenesis of liver cancer. Oncogene 2007; 26:2166–2176.
6. Loeb LA, Bielas JH, Beckman RA. Cancers exhibit a mutator phenotype: clinical implications. Cancer Res 2008;68:3551–3557.
7. Barrett MT, Sanchez CA, Prevo LJ, et al. Evolution of neoplastic cell lineages in Barrett oesophagus. Nat Genet 1999;22:106–109.
8. Leedham SJ, Graham TA, Oukrif D, et al. Clonality, founder mutations, and field cancerization in human ulcerative colitis-associated neoplasia. Gastroenterology 2009;136:542–550.
9. **Hussain SP, Hofseth LJ**, Harris CC. Radical causes of cancer. Nat Rev Cancer 2003;3:276–285.
10. Matsumoto Y, Marusawa H, Kinoshita K, et al. Helicobacter pylori infection triggers aberrant expression of activation-induced cytidine deaminase in gastric epithelium. Nat Med 2007;13:470–476.
11. Komori J, Marusawa H, Machimoto T, et al. Activation-induced cytidine deaminase links bile duct inflammation

to human cholangiocarcinoma. Hepatology 2008; 47:888–896.
12. Endo Y, Marusawa H, Kou T, et al. Activation-induced cytidine deaminase links between inflammation and the development of colitis-associated colorectal cancers. Gastroenterology 2008;135:889–898.
13. Ikeda K, Marusawa H, Osaki Y, et al. Antibody to hepatitis B core antigen and risk for hepatitis C-related hepatocellular carcinoma: a prospective study. Ann Intern Med 2007;146:649–656.
14. Endo Y, Marusawa H, Kinoshita K, et al. Expression of activation-induced cytidine deaminase in human hepatocytes via NF-kappaB signaling. Oncogene 2007; 26:5587–5595.
15. Kou T, Marusawa H, Kinoshita K, et al. Expression of activation-induced cytidine deaminase in human hepatocytes during hepatocarcinogenesis. Int J Cancer 2007; 120:469–476.
16. Wei X, Walia V, Lin JC, et al. Exome sequencing identifies GRIN2A as frequently mutated in melanoma. Nat Genet 2011;43:442–446.
17. Wang L, Tsutsumi S, Kawaguchi T, et al. Whole-exome sequencing of human pancreatic cancers and characterization of genomic instability caused by MLH1 haploinsufficiency and complete deficiency. Genome Res 2012;22:208–219.
18. **Wang K, Kan J**, Yuen ST, et al. Exome sequencing identifies frequent mutation of ARID1A in molecular subtypes of gastric cancer. Nat Genet 2011;43: 1219–1223.
19. **Fujimoto A, Totoki Y**, Abe T, et al. Whole-genome sequencing of liver cancers identifies etiological influences on mutation patterns and recurrent mutations in chromatin regulators. Nat Genet 2012;44:760–764.
20. **Guichard C, Amaddeo G, Imbeaud S**, et al. Integrated analysis of somatic mutations and focal copy-number changes identifies key genes and pathways in hepatocellular carcinoma. Nat Genet 2012;44:694–698.
21. Nasu A, Marusawa H, Ueda Y, et al. Genetic heterogeneity of hepatitis C virus in association with antiviral therapy determined by ultra-deep sequencing. PLoS One 2011;6:e24907.
22. Nishijima N, Marusawa H, Ueda Y, et al. Dynamics of hepatitis B virus quasispecies in association with nucleos(t)ide analogue treatment determined by ultra-deep sequencing. PLoS One 2012;7:e35052.
23. Varela I, Tarpey P, Raine K, et al. Exome sequencing identifies frequent mutation of the SWI/SNF complex gene PBRM1 in renal carcinoma. Nature 2011; 469:539–542.
24. **Clément K, Vaisse C**, Lahlou N, et al. A mutation in the human leptin receptor gene causes obesity and pituitary dysfunction. Nature 1998;392:398–401.
25. Laurent-Puig P, Zucman-Rossi J. Genetics of hepatocellular tumors. Oncogene 2006;25:3778–3786.
26. **Morita S, Matsumoto Y**, Okuyama S, et al. Bile acid-induced expression of activation-induced cytidine deaminase during the development of Barrett's oesophageal adenocarcinoma. Carcinogenesis 2011;32:1706–1712.
27. Lee GH, Proenca R, Montez JM, et al. Abnormal splicing of the leptin receptor in diabetic mice. Nature 1996; 379:632–635.
28. Becker FF. Thioacetamide hepatocarcinogenesis. J Natl Cancer Inst 1983;71:553–558.
29. Schnur J, Nagy P, Sebestyén A, et al. Chemical hepatocarcinogenesis in transgenic mice overexpressing mature TGF beta-1 in liver. Eur J Cancer 1999; 35:1842–1845.
30. Greenman C, Stephens P, Smith R, et al. Patterns of somatic mutation in human cancer genomes. Nature 2007;446:153–158.
31. **Yan XJ, Xu J, Gu ZH**, et al. Exome sequencing identifies somatic mutations of DNA methyltransferase gene DNMT3A in acute monocytic leukemia. Nat Genet 2011; 43:309–315.
32. Schwartz MW, Woods SC, Porte D, et al. Central nervous system control of food intake. Nature 2000;404:661–671.
33. Tartaglia LA. The leptin receptor. J Biol Chem 1997; 272:6093–6096.
34. **Peelman F, Iserentant H**, De Smet AS, et al. Mapping of binding site III in the leptin receptor and modeling of a hexameric leptin.leptin receptor complex. J Biol Chem 2006;281:15496–15504.
35. Farooqi IS, Wangensteen T, Collins S, et al. Clinical and molecular genetic spectrum of congenital deficiency of the leptin receptor. N Engl J Med 2007;356:237–247.
36. **Kimber W, Peelman F**, Prieur X, et al. Functional characterization of naturally occurring pathogenic mutations in the human leptin receptor. Endocrinology 2008; 149:6043–6052.
37. Yang S, Lin HZ, Hwang J, et al. Hepatic hyperplasia in noncirrhotic fatty livers: is obesity-related hepatic steatosis a premalignant condition? Cancer Res 2001; 61:5016–5023.
38. Marrero JA, Fontana RJ, Su GL, et al. NAFLD may be a common underlying liver disease in patients with hepatocellular carcinoma in the United States. Hepatology 2002;36:1349–1354.
39. Kodama Y, Brenner DA. c-Jun N-terminal kinase signaling in the pathogenesis of nonalcoholic fatty liver disease: multiple roles in multiple steps. Hepatology 2009;49:6–8.
40. Hourigan LF, Macdonald GA, Purdie D, et al. Fibrosis in chronic hepatitis C correlates significantly with body mass index and steatosis. Hepatology 1999;29:1215–1219.
41. Lonardo A, Adinolfi LE, Loria P, et al. Steatosis and hepatitis C virus: mechanisms and significance for hepatic and extrahepatic disease. Gastroenterology 2004; 126:586–597.
42. Ohata K, Hamasaki K, Toriyama K, et al. Hepatic steatosis is a risk factor for hepatocellular carcinoma in patients with chronic hepatitis C virus infection. Cancer 2003;97:3036–3043.
43. Cohen B, Novick D, Rubinstein M. Modulation of insulin activities by leptin. Science 1996;274:1185–1188.
44. Wang Y, Kuropatwinski KK, White DW, et al. Leptin receptor action in hepatic cells. J Biol Chem 1997; 272:16216–16223.

45. Elinav E, Abd-Elnabi A, Pappo O, et al. Suppression of hepatocellular carcinoma growth in mice via leptin, is associated with inhibition of tumor cell growth and natural killer cell activation. J Hepatol 2006;44:529–536.

Author names in bold designate shared co-first authorship.

Received February 11, 2013. Accepted September 10, 2013.

Reprint requests
Address requests for reprints to: Hiroyuki Marusawa, MD, PhD, Department of Gastroenterology and Hepatology, Graduate School of Medicine, Kyoto University, 54 Kawahara-cho, Shogoin, Sakyo-ku, Kyoto 606-8507, Japan. e-mail: maru@kuhp.kyoto-u.ac.jp; fax: (81) 75-751-4303.

Acknowledgments
Data profiling: Sequence reads with Genome Analyzer were deposited in the DNA Data Bank of Japan Sequence Read Archive (http://trace.ddbj.nig.ac.jp/dra/index_e.shtml) under accession no. DRA000867.

The authors thank Dr K. Terasawa, Dr T. Fujiwara, Dr K. Takahashi, and Dr Y. Ueda for helpful suggestions; Dr N. Nishijima, Dr A. Takai, Dr A. Nasu, Dr Y. Endo, Y. Nakagawa, and C. Kakimoto for help with the analyses; and Dr H. Kokuryu and Dr T. Kusaka at Kyoto Katsura Hospital for their support.

Conflicts of interest
The authors disclose no conflicts.

Funding
Supported by Japan Society for the Promotion of Science Grants-in-Aid for Scientific Research, KAKENHI on Innovative Areas, and Health and Labour Sciences Research Grants for Research on Intractable Disease and Research on Hepatitis from the Ministry of Health, Labour and Welfare, Japan.

Supplementary Methods

Patients

The study group comprised patients who underwent living donor liver transplantation or potentially curative resection of primary HCC at Kyoto University Hospital from 2000 to 2010. The selection of patients enrolled in this study was based on the availability of a sufficient amount of tissue for analysis. Patients included 17 men and 9 women, with a mean age at the time of surgery of 54.9 ± 7.7 years (mean ± SD; range, 37–76 years). Among them, whole exome sequencing was applied to 7 tumors, 4 nontumorous cirrhotic livers, and matched peripheral lymphocytes from 4 patients (Supplementary Table 1, patients 1–4). Furthermore, we performed selected exome sequencing of 22 nontumorous cirrhotic livers, 10 tumors, and matched peripheral lymphocytes from 22 other affected patients (Supplementary Table 1, patients 5–26). All patients were positive for serum anti-HCV and/or HCV RNA. Written informed consent for the use of resected tissue was obtained from all patients in accordance with the Declaration of Helsinki, and the Kyoto University Graduate School and Faculty of Medicine Ethics Committee approved the study.

Sequence Data Analysis and Variant Filtering

Using NextGENe v2.2 software (SoftGenetics, State College, PA), the obtained reads were aligned with the reference sequences of the Human Genome Build 37.3. Reads with 96% or more bases matching a particular position of the reference sequences were aligned. Furthermore, reads with a median quality value score of more than 20 and no more than 3 uncalled nucleotides were allowed anywhere in one read. Only sequences that passed the quality filters were analyzed, and each position of the genome was assigned a coverage depth representing the number of times the nucleotide position was sequenced. To identify somatic mutations, we used a number of scores to provide an empirical estimation of the likelihood that a given mutation was real and not an artifact of sequencing or alignment errors.

In the whole exome sequencing analysis, candidates of somatic mutations were selected according to the variant filtering process (Supplementary Figure 1). We defined nucleotide alterations that appeared in more than 20% of reads as somatic mutations.[1–3] When detecting the genes commonly mutated in both tumor and nontumorous liver tissues of the same subjects, we also selected potential nucleotide alterations that appeared between 5% and 20% of the total reads in nontumorous liver tissues for further evaluation. We excluded potential somatic mutations that represented more than 5% of the reads in peripheral lymphocytes of the same patient as common variants in each individual. Candidate nucleotide alterations were tested using standard Sanger sequencing on an Applied Biosystems 3500 Genetic Analyzer (Applied Biosystems, Foster City, CA) to validate the presence of each mutation.

In selected exome sequencing analysis, candidates of somatic mutations were selected according to the variant filtering process (Supplementary Figure 2). We defined somatic mutations with more than 20% of reads as high-frequency mutations and those that appeared between 1% and 20% of total reads as low-frequency mutations. We excluded potential somatic mutations that represented more than 1% of the reads in peripheral lymphocytes of the same patient. In cases in which we could not obtain lymphocyte DNA, candidates of somatic mutations found in the lymphocytes of 2 or more different patients were excluded in consideration of possible Japanese polymorphisms.

We compared our variants against common and germline polymorphisms present in the dbSNP135 to discard known germline single nucleotide polymorphisms.

All sequence reads were deposited in the DNA Data Bank of Japan Sequence Read Archive (accession no. DRA000867).

Score

SoftGenetics developed the overall mutation score to provide an empirical estimation of the likelihood that a given mutation is real and not an artifact of sequencing or alignment errors. The overall mutation score of NextGENe can be used like Phred scores, in which the scores are logarithmically linked to error probabilities. The overall mutation score of NextGENe is obtained as the product of the "coverage score," which is calculated from the depth of coverage at the position of the mutation and with a value ranging from 0 (where depth of coverage is 1) to an unlimited number, multiplied by each of the 4 types of additional penalty scores, such as the read balance score, allele balance score, mismatch score, and wrong allele score, with values less than 1 but positive (the calculating formula for each score is not shown). These scores are described in the NextGENe User Manual in detail (http://www.softgenetics.com/NextGENe.html).

Overall mutation score. SoftGenetics developed the overall mutation score to provide an empirical estimation of the likelihood that a given mutation is real and not an artifact of sequencing or alignment errors. A low overall mutation score, however, does not mean that the mutation is more than likely a false mutation. The low score implies only that the mutation cannot be called a true mutation with absolute certainty. As a general guideline, if the coverage is high (500 to several thousand reads) and the data are bidirectional, then scores that are ≤ 5 indicate that the mutation is most likely false, whereas scores of ≥ 25 indicate that the mutation is most likely true.

Mismatch score. Several variations from the reference sequence that occur very close together often indicate a region where mutation calls are less reliable. The mismatch score penalizes a specific mutation if other mismatched bases are found nearby. The software first looks for mismatches that occur in a minimum percentage of reads in the 10-base pair region that is found on either side of the mutation that is being scored.

Wrong allele score. Mismatches that are different from the consensus are referred to as wrong mismatches. These wrong mismatches most likely result from sequencing errors. For example, A, C, G, T, and insertions represent wrong mismatches when a deletion was called at a position.

Cell Culture and Transfection

The complementary DNA encoding the wild-type and the mutated LEPR were generated by reverse-transcription polymerase chain reaction from the messenger RNA of the liver tissues, followed by polymerase chain reaction amplification using Phusion high-fidelity DNA polymerase (Finnzymes, Espoo, Finland) and the following oligonucleotide primers: 5′-CGCGGATCCATGATTTGTCAAAAATTC-3′ (sense) and 5′- AAGGAAAAAAGCGGCCGCTTACACAGTTAGGTCA CACA-3′ (antisense). The resulting polymerase chain reaction fragments were inserted into the *Bam*HI-*Not*I sites of pcDNA3 for HEK293 and the *Bam*HI-*Apa*I sites of lentivirus for HepG2, as described previously.[4]

HEK293 and HepG2 cells were maintained in Dulbecco's modified Eagle medium (Gibco BRL, Rockville, MD) containing 10% fetal bovine serum. For transfection of plasmids into HEK293 cells, we used Lipofectamine2000 transfection reagent (Invitrogen, Carlsbad, CA). At 40 hours after transfection, the cells were serum starved for 8 hours and then either left unstimulated or stimulated with 100 ng/mL recombinant human leptin (Sigma-Aldrich, St Louis, MO) for 10 minutes. Expression of either wild-type or mutant LEPR in HepG2 cells was performed using a lentiviral vector–mediated wild-type and mutated LEPR expression system as described previously.[5] In brief, LEPR complementary DNA fragments were inserted into the viral vectors, followed by the production of lentiviral stocks in HEK293 cells. HepG2 cells were cultured in virus-containing medium for 48 hours, starved for 8 hours, treated with 100 ng/mL recombinant human leptin (Sigma-Aldrich) for 10 minutes, and then subjected to immunoblotting, immunostaining, quantitative reverse-transcription polymerase chain reaction, or a cell proliferation (3-[4,5-dimethylthiazol-2-yl]-2,5-diphenyltetrazolium bromide [MTT]) assay.

Immunoblotting Analysis

Immunoblotting was performed using anti-STAT3 and anti–phospho-STAT3 antibody (Cell Signaling Technology, Danvers, MA) according to the manufacturer's protocol.

Animal Experiments

C57BL/KsJ-*db/db* mice (*db/db* mice), which possess homozygous deletion of the *Lepr*, *Ob-R* gene, and misty mice, which are wild-type with a normal *Lepr*, were purchased from Japan SLC (Shizuoka, Japan). TAA (Sigma-Aldrich) was prepared at a concentration of 0.02% and administered in drinking water to mice for 24 weeks or 30 weeks beginning at 5 weeks of age. These mice were then killed for analysis of the development of liver tumors. All animal experiments were approved by the Ethics Committee for Animal Experiments and performed under the Guidelines for Animal Experiments of Kyoto University.

Supplementary References

1. **Wang K, Kan J**, Yuen ST, et al. Exome sequencing identifies frequent mutation of ARID1A in molecular subtypes of gastric cancer. Nat Genet 2011;43:1219–1223.
2. Varela I, Tarpey P, Raine K, et al. Exome sequencing identifies frequent mutation of the SWI/SNF complex gene PBRM1 in renal carcinoma. Nature 2011;469:539–542.
3. **Yan XJ, Xu J, Gu ZH**, et al. Exome sequencing identifies somatic mutations of DNA methyltransferase gene DNMT3A in acute monocytic leukemia. Nat Genet 2011; 43:309–315.
4. Endo Y, Marusawa H, Kinoshita K, et al. Expression of activation-induced cytidine deaminase in human hepatocytes via NF-kappaB signaling. Oncogene 2007; 26:5587–5595.
5. **Morita S, Matsumoto Y**, Okuyama S, et al. Bile acid-induced expression of activation-induced cytidine deaminase during the development of Barrett's oesophageal adenocarcinoma. Carcinogenesis 2011;32:1706–1712.
6. Aly HH, Watashi K, Hijikata M, et al. Serum-derived hepatitis C virus infectivity in interferon regulatory factor-7-suppressed human primary hepatocytes. J Hepatol 2007;46:26–36.

Supplementary Table 1. Clinical Features of 4 Patients Who Underwent Whole Exome Sequencing and 22 Patients Who Underwent Selected Exome Sequencing

Patient no.	Age (*y*)	Sex	Body mass index (*kg/m²*)	α-Fetoprotein (*ng/mL*)	Des-γ-carboxy prothrombin (*mAU/mL*)	HCC	Histological grade
Whole exome sequencing							
1	51	Male	23.3	16	185	M	Well
2	58	Female	22.3	103	7	M	Mod
3	55	Female	26.7	779	881	M	Mod
4	53	Male	22.3	34	85	S	Mod
Selected exome sequencing							
5	65	Male	25.2	17	7	M	Mod
6	49	Female	21.6	149	107	M	Mod
7	40	Male	25.7	24	50	M	Mod
8	50	Male	25.0	16	23	M	Mod
9	57	Female	23.4	8	30	M	Mod
10	56	Female	22.8	5	929	M	Mod
11	53	Male	18.6	30	31	M	Mod
12	65	Female	29.7	6	1877	S	Mod
13	57	Male	19.0	19	167	S	Well
14	76	Male	21.8	75,363	37,784	M	Poor
15	64	Male	18.7	177	8	—	—
16	57	Male	25.5	45	68	—	—
17	54	Female	25.9	<3	10	—	—
18	50	Male	22.3	585	61	—	—
19	60	Female	21.3	434	72	—	—
20	57	Male	25.0	15	8310	—	—
21	56	Male	19.0	15	383	—	—
22	49	Female	21.8	38	227	—	—
23	59	Male	25.6	6	12	—	—
24	49	Male	23.2	4	320	—	—
25	37	Male	22.2	4	13	—	—
26	51	Male	20.5	3	90	—	—

M, multiple; Well, well-differentiated HCC; Mod, moderately differentiated HCC; S, solitary; Poor, poorly differentiated HCC.

Supplementary Table 2. Overview of Whole Exome Sequencing Data From 4 Patients With HCC Who Had HCV Infection

	Tumor (n = 7)	Nontumor (n = 4)	Lymphocytes (n = 4)
Total reads	44,323,036	41,920,372	38,661,394
Aligned reads	40,046,800	33,742,449	31,595,571
Aligned sequence (*base pairs*)	2,824,088,514	2,384,058,470	2,221,753,713
Median read depth	40.2	31.9	27.4
Coverage			
1×	31,560,125	32,343,635	30,935,484
8×	24,724,702	23,432,758	23,549,909
20×	17,707,636	15,000,474	16,272,508
30×	13,599,418	11,752,775	12,527,511

NOTE. Whole exome sequencing was performed on tumor tissues, nontumorous cirrhotic liver tissues, and matched peripheral lymphocytes from each patient. Total reads, aligned reads, aligned sequences (base pairs), median read depth, and number of target regions, which were 1×, 8×, 20×, and 30× or more coverage depth read, are shown.